SUPPORTING INFORMATION

High thermal durability of layered $Cs_4Co^{II}[W^V(CN)_8]Cl_3$ framework: crystallographic and ^{133}Cs NMR spectroscopic studies

Koji Nakabayashi,[†] Szymon Chorazy,[†] Yasuto Miyamoto,[†] Takashi Fujimoto,[†] Koji Yazawa,[§] Daisuke Takahashi,[†] Barbara Sieklucka,[‡] and Shin-ichi Ohkoshi[*,†]*

†Department of Chemistry, School of Science, The University of Tokyo, 7-3-1 Hongo, Bunkyo-ku, Tokyo 113-0033, Japan.

‡Faculty of Chemistry, Jagiellonian University, Ingardena 3, 30-060 Kracow, Poland.

§JEOL RESONANCE Inc., 1-2, Musashino 3-Chome, Akishima, Tokyo 196-8558, Japan.

Table S1. Crystal data and structure refinements at respective temperatures.

Temperature		**300 K**	**400 K**	**473 K**
method		single-crystal XRD	single-crystal XRD	single-crystal XRD
formula		$Cs_4Co_1W_1Cl_3C_8N_8$	$Cs_4Co_1W_1Cl_3C_8N_8$	$Cs_4Co_1W_1Cl_3C_8N_8$
formula weight [g·mol^{-1}]		1088.93	1088.93	1088.93
T [K]		300(2)	400(2)	473(2)
λ [Å]		0.68890	0.68890	0.68890
crystal system		monoclinic	monoclinic	monoclinic
space group		$P\,2_1/n$	$P\,2_1/n$	$P\,2_1/n$
unit cell	a	9.397(1)	9.427(1)	9.450(1)
	b	13.751(1)	13.785(1)	13.796(1)
	c	16.804(1)	16.814(1)	16.753(1)
	β	95.736(1)	95.667(1)	95.654(1)
V [Å^3]		2160.5(3)	2174.1(3)	2173.5(3)
Z		4	4	4
calculated density [g·cm^{-3}]		3.348	3.326	3.328
absorption coeff. [cm^{-1}]		13.110	13.027	13.032
F(000)		1904	1904	1904
crystal size [mm × mm × mm]		0.08 × 0.06 × 0.02	0.08 × 0.06 × 0.02	0.08 × 0.06 × 0.02
Θ range [deg]		2.31 – 32.32	1.86 – 32.36	1.86 – 32.36
limiting indices		$-14 < h < 14$ $-21 < k < 21$ $-26 < l < 26$	$-12 < h < 14$ $-21 < k < 21$ $-24 < l < 25$	$-14 < h < 14$ $-19 < k < 19$ $-21 < l < 25$
collected reflections		45418	22865	19696
unique reflections		8425	8409	7745
R_{int}		0.0736	0.0772	0.1133
max and min transmission		0.7795 and 0.4202	0.7806 and 0.4221	0.7806 and 0.4220
refinement method		full-matrix least-squares on F^2	full-matrix least-squares on F^2	full-matrix least-squares on F^2
data/parameters/restraints		8425/226/0	8409/226/0	7745/226/0
GOF on F^2		0.972	0.877	0.949
final R indices		$R_1 = 0.0278$ [$I > 2\sigma(I)$] $wR_2 = 0.0645$ (all data)	$R_1 = 0.0414$ [$I > 2\sigma(I)$] $wR_2 = 0.0945$ (all data)	$R_1 = 0.0733$ [$I > 2\sigma(I)$] $wR_2 = 0.1806$ (all data)
largest diff peak and hole		1.707 and -2.407 e·A^{-3}	1.599 and -4.272 e·A^{-3}	2.609 and -3.524 e·A^{-3}

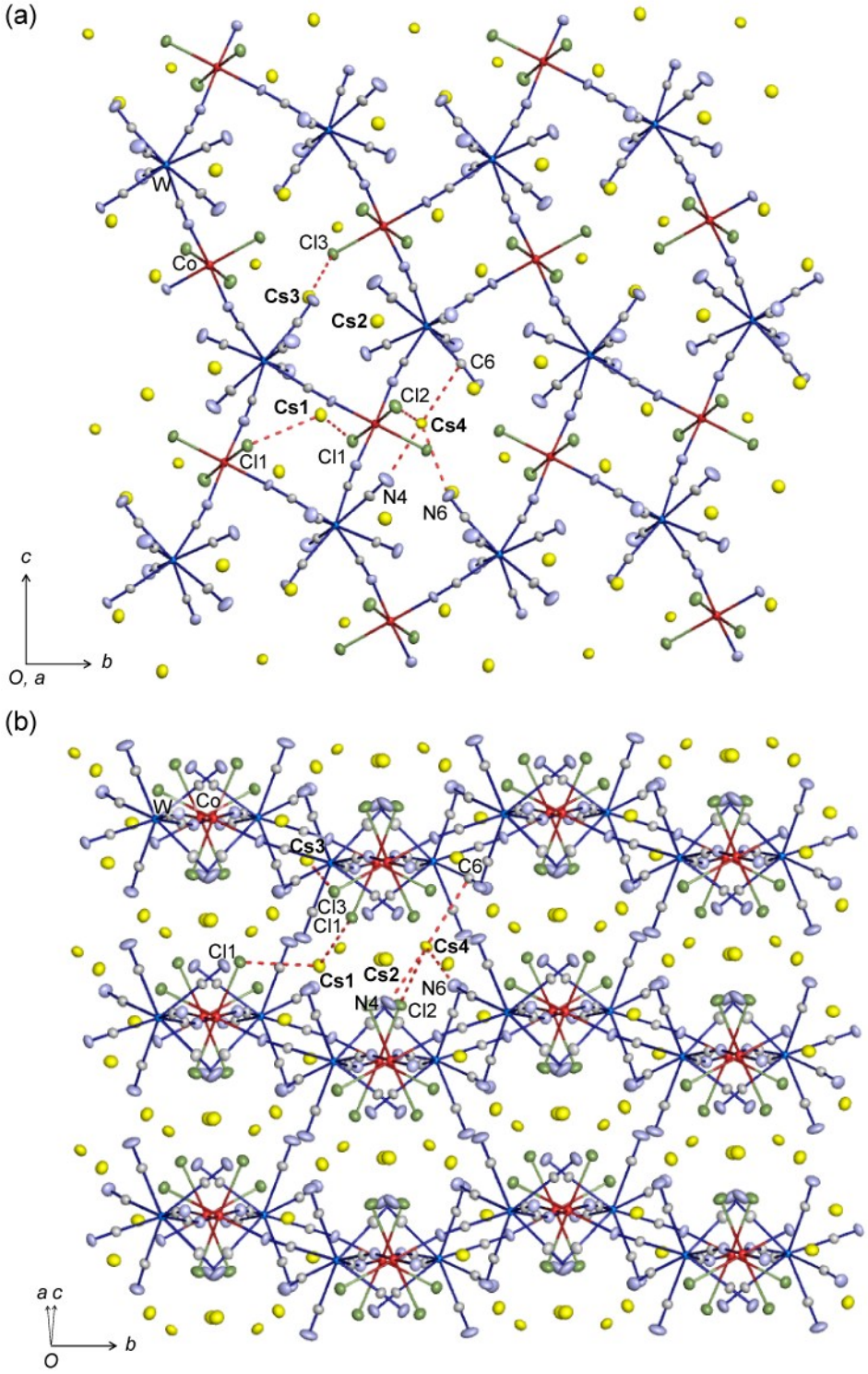

Fig. S1. The crystal structure with thermal ellipsoids at 400 K: (a) the view along *a* axis and (b) the view along a diagonal line. The thermal ellipsoids are shown as 30% probability. The red dashed lines represent the weak bonds between the Cs^+ ions and contact atoms.

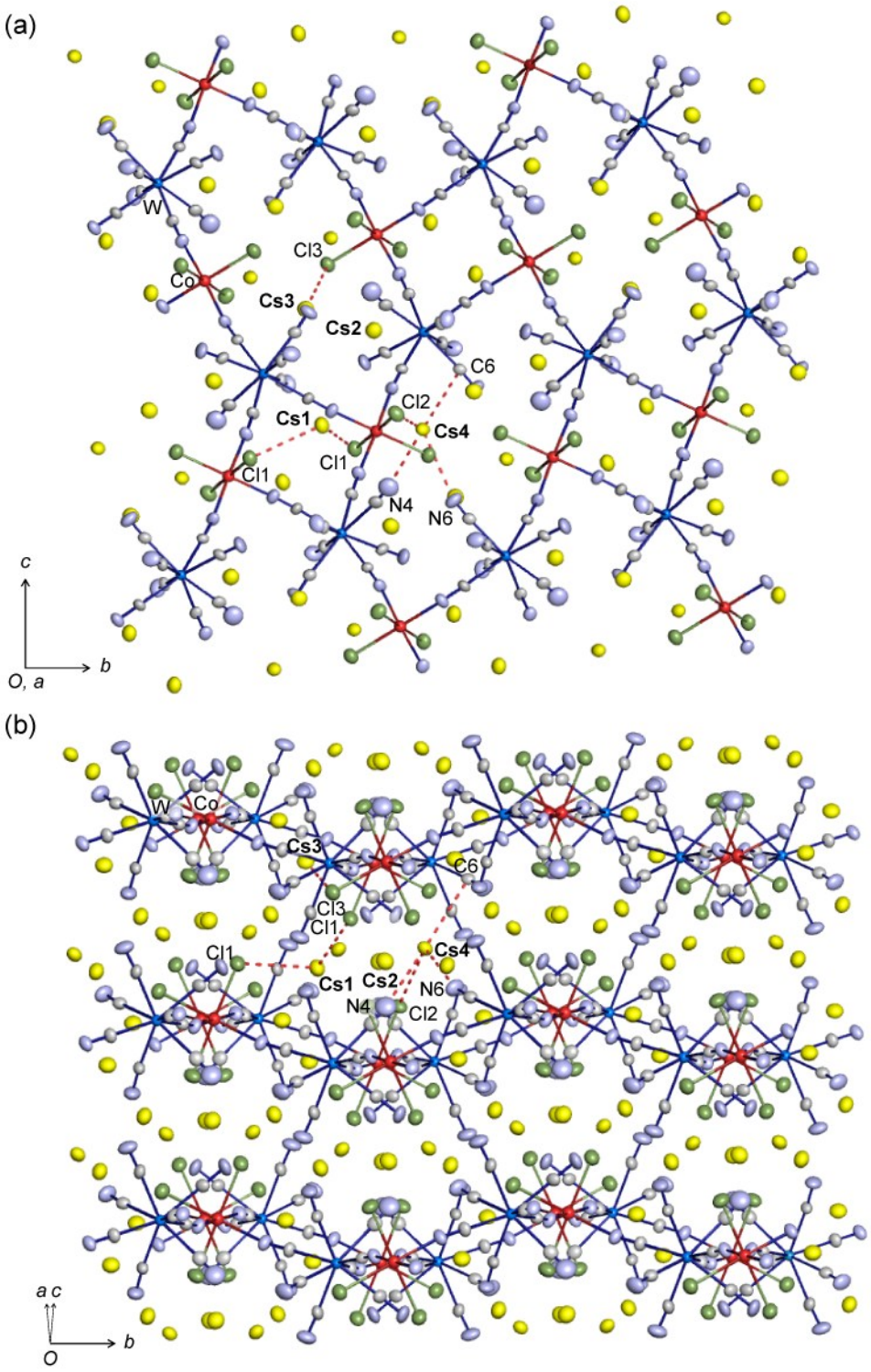

Fig. S2. The crystal structure with thermal ellipsoids at 473 K: (a) the view along *a* axis and (b) the view along a diagonal line. The thermal ellipsoids are shown as 30% probability. The red dashed lines represent the weak bonds between the Cs^+ ions and contact atoms.

Table S2. The representative distances between Cs^+ ions and neighbor atoms at respective temperatures. The bold ones show shorter distances than the estimated sum of an ionic radius of Cs^+ ion (1.74 Å) and a van der Waals radius of N (1.55 Å) (or C (1.70 Å)) or Cl- ionic radius (1.81 Å), that is, 3.55 Å for $Cs^+\cdots Cl^-$, 3.29 Å for $Cs^+\cdots N$, and 3.44 Å for $Cs^+\cdots C$.

Atom name		300 K	400 K	473 K
Cs1	C7	3.783	3.798	3.780
	N3	3.807	3.808	3.788
	N5	**3.281**	3.309	3.316
	N7	3.474	3.472	3.430
	N8	3.309	3.316	3.338
	Cl1	**3.454**	**3.470**	**3.483**
	Cl1'	**3.524**	**3.518**	**3.530**
	Cl2	3.805	3.815	3.817
Cs2	N3	3.780	3.832	3.879
	N4	3.562	3.579	3.638
	N5	3.386	3.391	3.401
	N6	3.412	3.438	3.475
	N8	3.479	3.494	3.506
	Cl1	3.566	3.582	3.609
	Cl2	3.712	3.707	3.676
	Cl3	3.644	3.654	3.668
Cs3	N4	3.592	3.591	3.590
	N5	3.537	3.537	3.506
	N6	3.459	3.468	3.454
	N7	3.292	3.316	3.342
	N8	3.349	3.341	3.355
	Cl2	**3.544**	3.554	3.590
	Cl3	**3.416**	**3.421**	**3.433**
	Cl3'	3.666	3.683	3.736
Cs4	C6'	**3.406**	**3.421**	**3.401**
	N4	**3.000**	**3.013**	**3.081**
	N6	**3.269**	**3.269**	**3.289**
	N6'	3.313	3.320	3.325
	Cl1	**3.538**	3.550	3.550
	Cl2	**3.468**	**3.476**	**3.454**
	Cl3	3.595	3.615	3.629
	Cl3'	3.648	3.668	3.670

Table S3. The distances between neighbor Cs^+ ions at respective temperatures.

Atom name		300 K	400 K	473 K
Cs1	Cs1'	5.037	5.036	5.044
	Cs2	4.957	4.980	5.017
	Cs2'	5.188	5.188	5.155
	Cs3	5.308	5.305	5.267
	Cs4	4.401	4.411	4.422
	Ave.	4.978	4.984	4.981
Cs2	Cs1	4.957	4.980	5.017
	Cs1'	5.188	5.188	5.155
	Cs3	5.048	5.050	5.037
	Cs3'	5.073	5.076	5.060
	Cs4	4.790	4.795	4.810
	Ave.	5.011	5.018	5.016
Cs3	Cs1	5.308	5.305	5.267
	Cs2	5.048	5.050	5.037
	Cs2'	5.073	5.076	5.060
	Cs3'	4.570	4.587	4.652
	Cs4	4.561	4.579	4.592
	Cs4'	5.055	5.056	5.062
	Ave.	4.936	4.942	4.945
Cs4	Cs1	4.401	4.411	4.422
	Cs2	4.790	4.795	4.810
	Cs3	4.561	4.579	4.592
	Cs3'	5.055	5.056	5.062
	Cs4	4.202	4.216	4.232
	Ave.	4.602	4.611	4.624

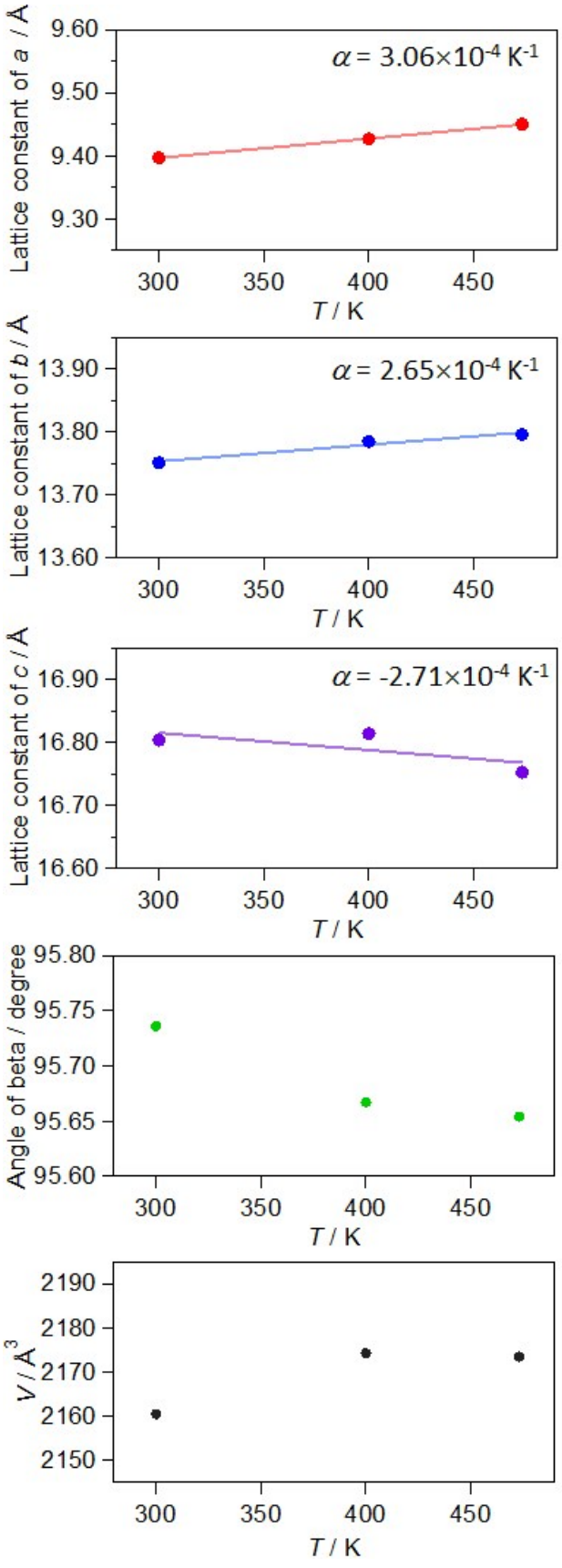

Fig. S3. The temperature dependency of the crystal parameters. The values of α represent the linear expansion coeficients.

Table S4. The distances of coordination bonds around Co^{II} and W^{V} at respective temeratures.

Atom name		300 K	400 K	473 K
Co1	N1	2.126	2.128	2.129
	N2	2.141	2.143	2.136
	N3	2.129	2.136	2.131
	Ave.	2.132	2.136	2.132
	Cl1	2.451	2.452	2.463
	Cl2	2.448	2.445	2.454
	Cl3	2.500	2.507	2.521
	Ave.	2.466	2.468	2.479
W1	C1	2.167	2.170	2.177
	C2	2.159	2.166	2.174
	C3	2.167	2.168	2.157
	C4	2.133	2.141	2.222
	C5	2.159	2.160	2.154
	C6	2.158	2.162	2.227
	C7	2.165	2.165	2.183
	C8	2.173	2.167	2.172
	Ave.	2.160	2.162	2.183

Table S5. The shortest distances between Cs^{+}-Co^{II} and Cs^{+}-W^{V} at respective temeratures.

Atom name		300 K	400 K	473 K
Co1	Cs1	4.666	4.670	4.642
	Cs2	4.450	4.478	4.522
	Cs3	4.526	4.543	4.598
	Cs4	4.445	4.476	4.514
W1	Cs1	4.938	4.936	4.894
	Cs2	5.112	5.123	5.108
	Cs3	5.033	5.042	5.040
	Cs4	4.305	4.327	4.334

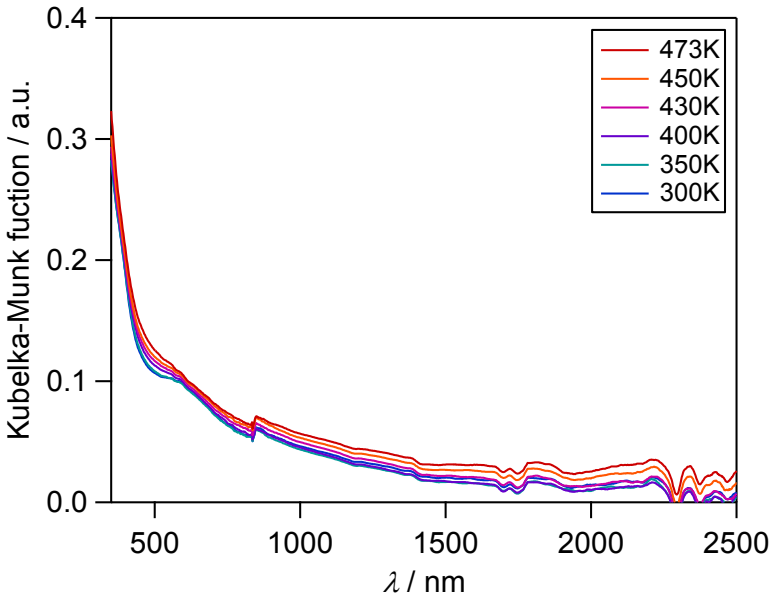

Fig. S4. Temperature dependence of the UV-vis absorption spectra for $Cs_4Co^{II}[W^{V}(CN)_8]Cl_3$ measured at 300K, 350K, 400K, 430K, 450K, and 473K. These absorption spectra are measured in the reflectance mode, and the scattering effect due to microcrystals is also included.

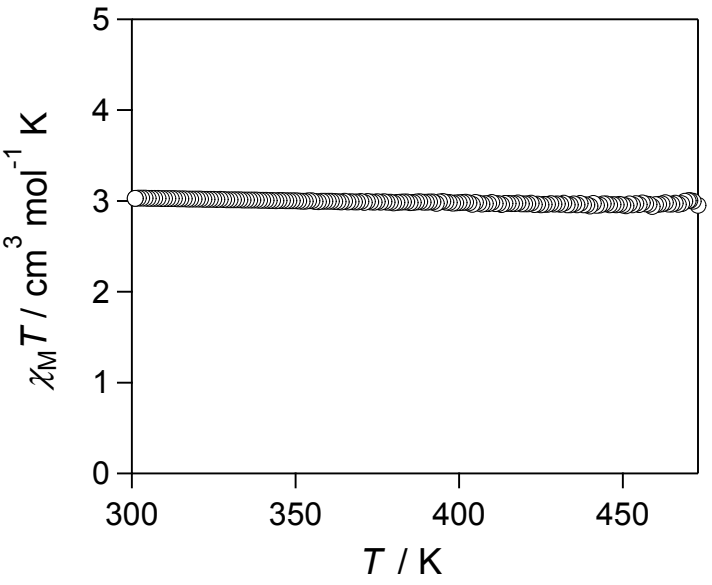

Fig. S5. Temperature dependence of $\chi_M T$ in the applied field of 5 kOe.

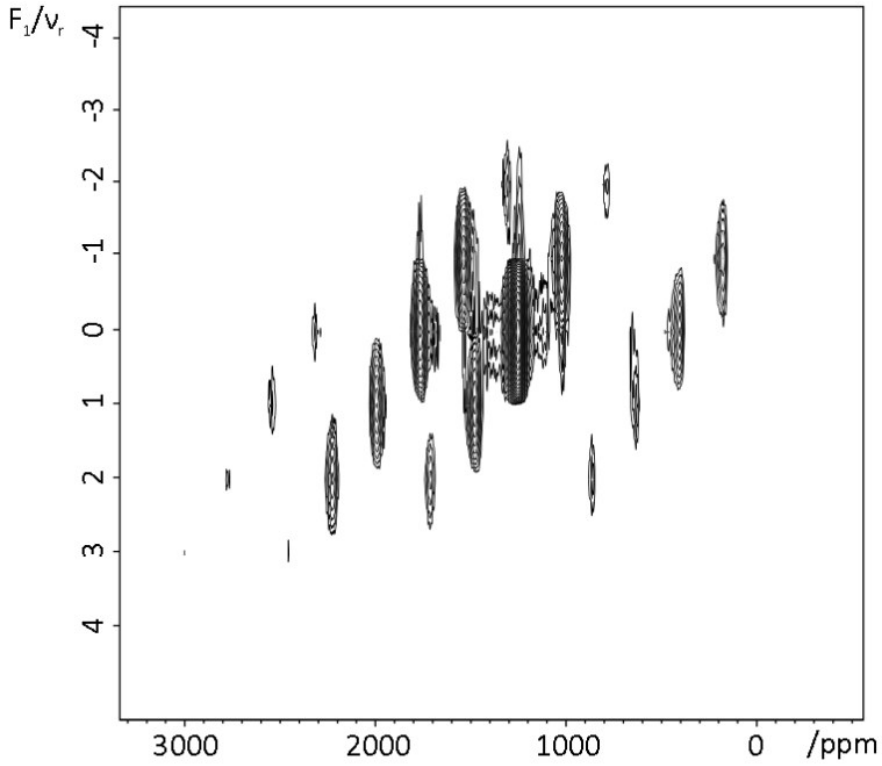

Fig. S6. 2D MATPSS spectrum at 331 K. The measurements was carried out by using an extended-VT 3.2 mm MAS probe. The experimental conditions were set up with the ^{133}Cs rf field strength for the excitation of 62.5 kHz (pulse length = 4 μs), recycle delay of 0.1 s, 8 t1 points with 4000 scans per point, and MAS rate of 18 kHz. The temperature of sample was also calibrated by $Pb(NO_3)_2$.